Electronic Supplementary Material (ESI) for Journal of Materials Chemistry A.


*Supplementary Information*

# A high-performance $TiO_2$ protective layers derived from non-high vacuum technology for Si-based photocathode to enhance photoelectrochemical water splitting

Xin Li[a], Hui Zhao[a], Jie Huang[a], Ying Li*[a], Hongyan Miao[a], Gang Shi*[a], Po Keung Wong[b]

[a] The Key Laboratory of Synthetic and Biotechnology Colloids, Ministry of Education, School ofChemical and Material Engineering, Jiangnan University, Wuxi 214122, China

[b] School of Life Sciences, The Chinese University of Hong Kong, Shatin, NT, Hong Kong, SAR, China

*E-mail: liying@jiangnan.edu.cn, gangshi@jiangnan.edu.cn

**Fig. S1** Optical image for photoelectrochemical hydrogen evolution reaction device.

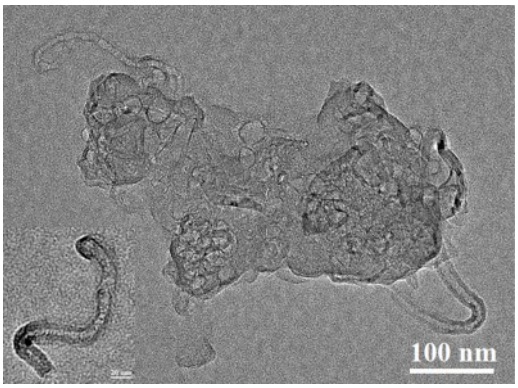


**Fig. S2** TEM image of Co-NCNHP derived from ZIF-8@ZIF-67.

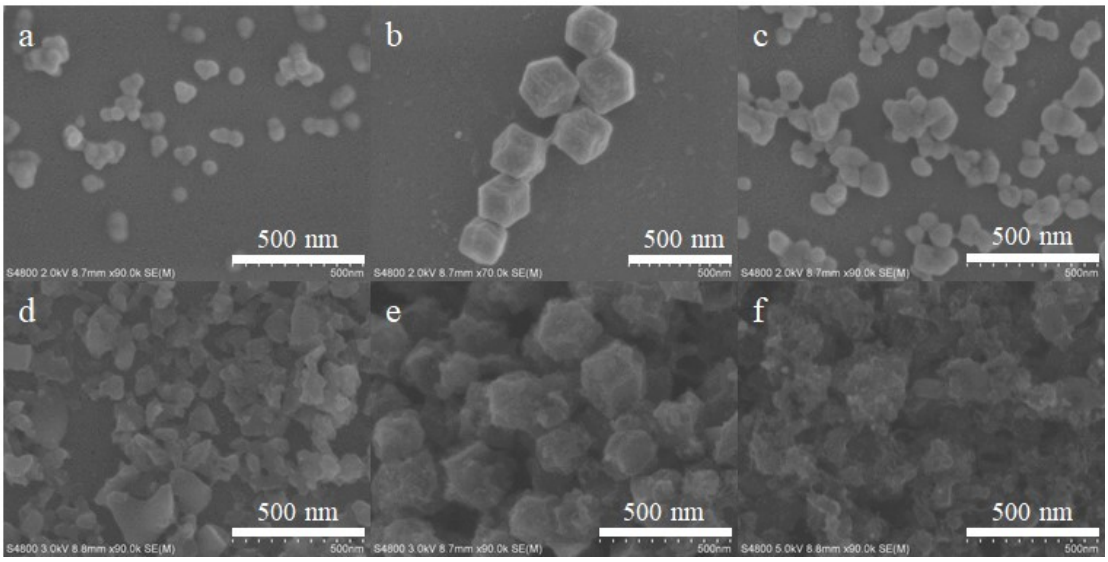


**Fig. S3** SEM images of ZIF-8 (a), ZIF-67 (b), ZIF-8@ZIF-67 (c), ZIF-8-derived NCP (d), ZIF-67-derived Co-NCP (e) and ZIF-8@ZIF-67 derived Co-NCNHP (f).

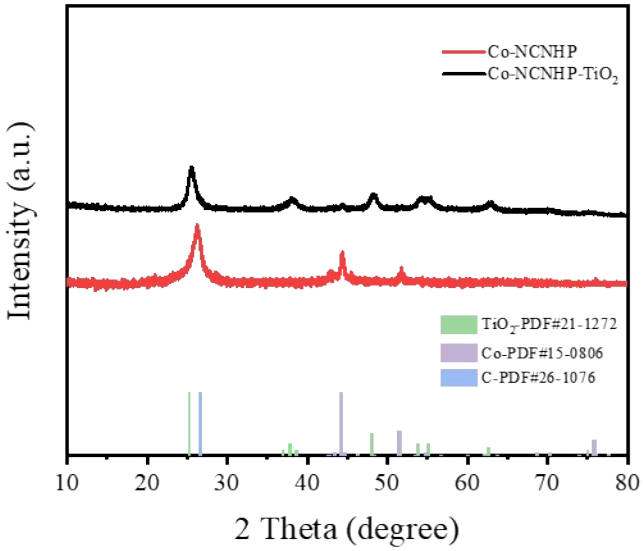


**Fig. S4** XRD patterns of Co-NCNHP and Co-NCNHP-$TiO_2$.

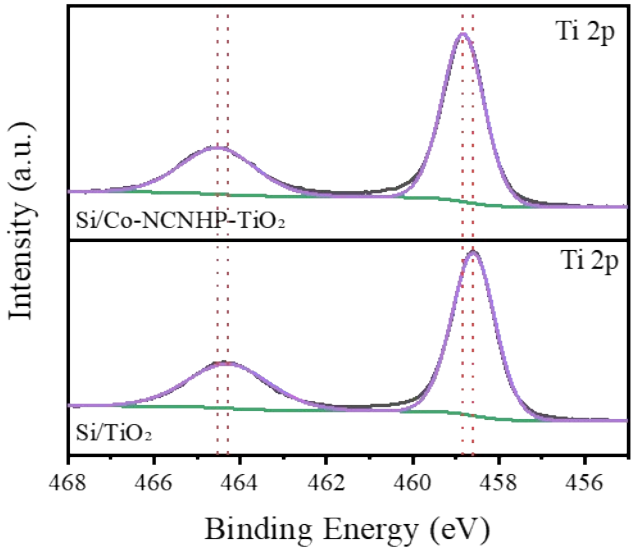


**Fig. S5** High-resolution Ti 2p spectra of Si/Co-NCNHP-$TiO_2$ and Si/$TiO_2$.

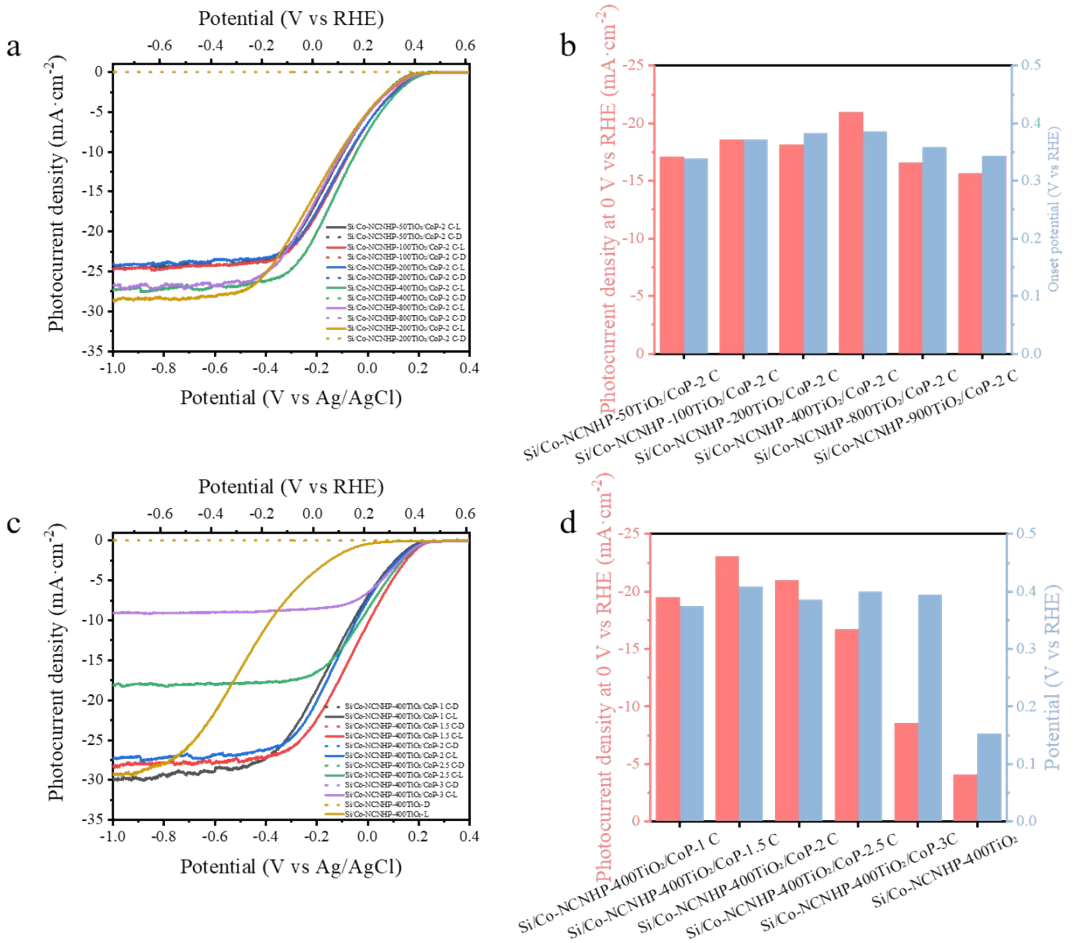


**Fig. S6** LSV curves, onset potential and photocurrent density at 0 V vs RHE for samples with different Co-NCNHP to $TiO_2$ ratios (a, b) and CoP loadings (c, d) under 1 solar irradiation in 0.5 M $H_2SO_4$. Where # and & in Si/Co-NCNNHP-# $TiO_2$/CoP-& C represent the volume ratio of Co-NCNHP dispersion to $TiO_2$ solution in the precursor of 1000-#: # and the charge density of CoP photodeposition (& C·cm$^{-2}$), respectively. In this paper, if not otherwise specified, Si/Co-NCNHP-$TiO_2$/CoP is denoted as Si/Co-NCNHP-400$TiO_2$/CoP-1.5 C.

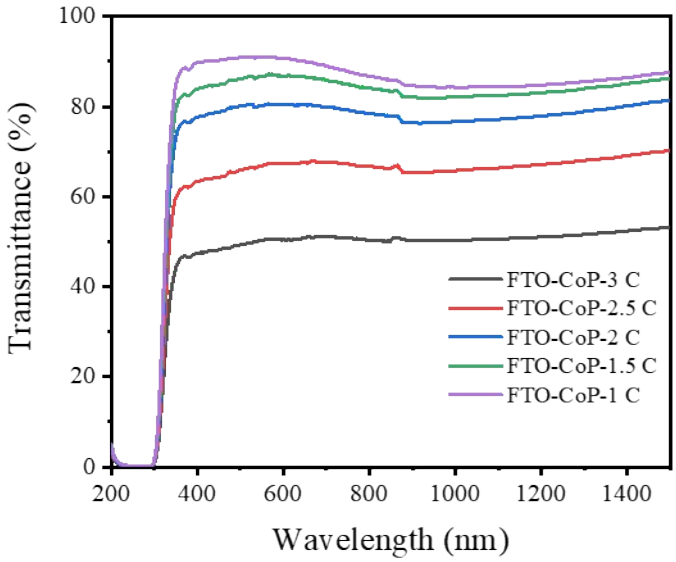


**Fig. S7** Transmission spectra of different amounts of CoP loaded on FTO.

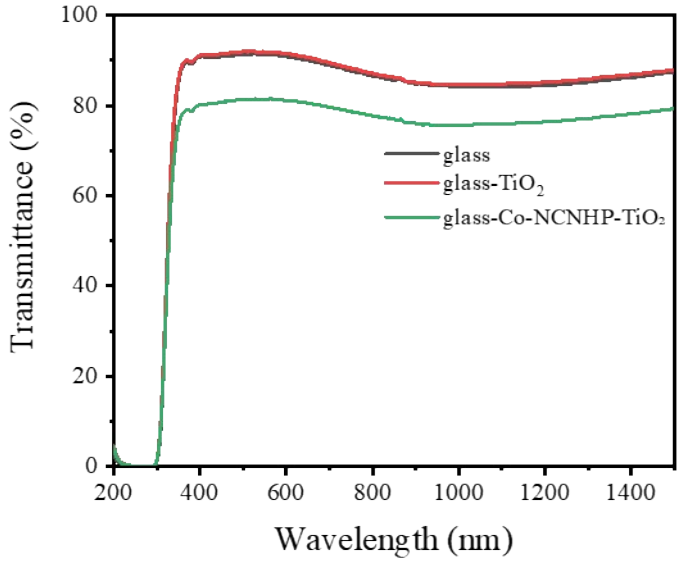


**Fig. S8** Transmission spectra of glass, glass-$TiO_2$ and glass-Co-NCNHP-$TiO_2$.

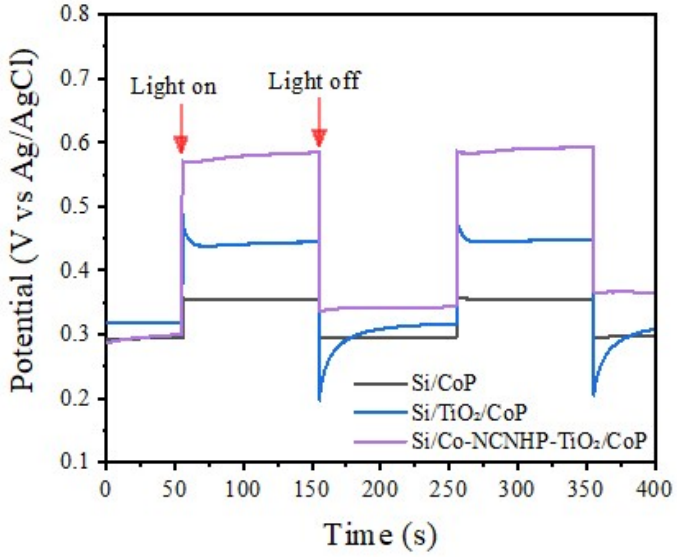


**Fig. S9** Open circuit potential (OCP) measurements of Si/Co-NCNHP-$TiO_2$/CoP, Si/$TiO_2$/CoP, and Si/CoP photocathodes under chopped light irradiation. photovoltage: $V_{ph}=V_{light}-V_{dark}$.

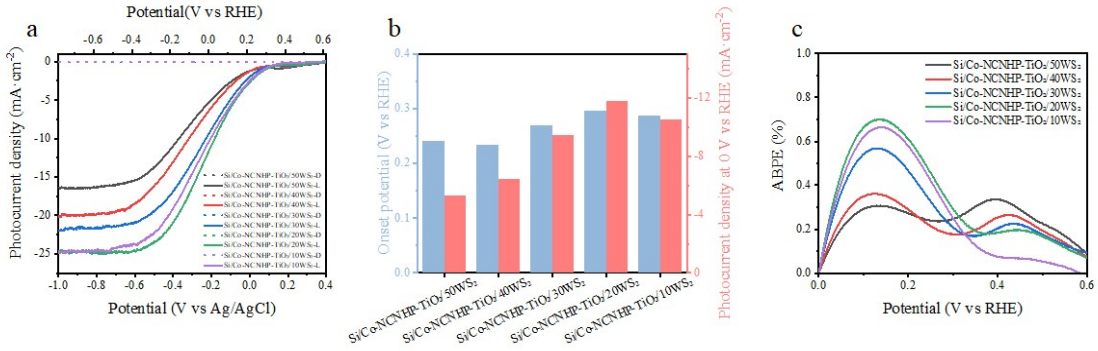


**Fig. S10** (a) LSV curves, (b) onset potential and photocurrent density at 0 V vs RHE, (c) ABPE for samples with different $WS_2$ loading under 1 solar irradiation in 0.5 M $H_2SO_4$. Where ξ in Si/Co-NCNHP-$TiO_2$/ξ $WS_2$ represents the concentration of $(NH_4)_2WS_4$ in the precursor solution (ξ mM). In this paper, if not otherwise specified, Si/Co-NCNHP-$TiO_2$/$WS_2$ is denoted as Si/Co-NCNHP-$TiO_2$/20$WS_2$.

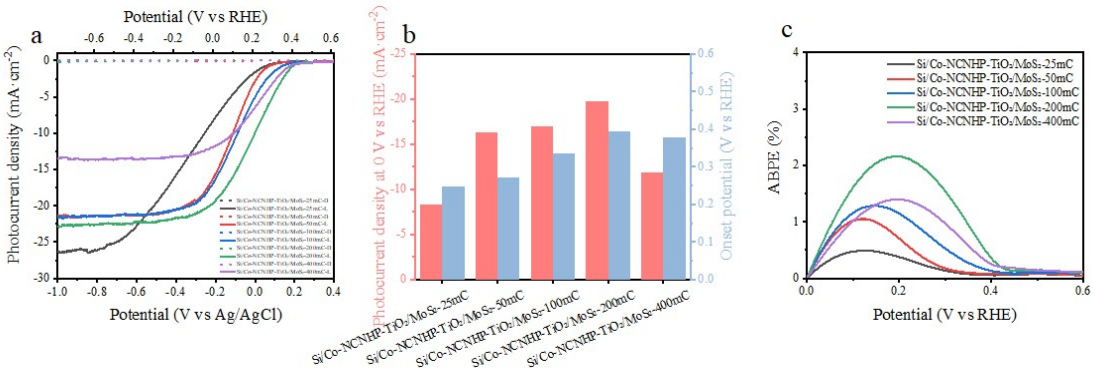


**Fig. S11** (a) LSV curves, (b) onset potential and photocurrent density at 0 V vs RHE, (c) ABPE for samples with different $MoS_2$ loading under 1 solar irradiation in 0.5 M $H_2SO_4$. Where ※ in Si/Co-NCNHP-$TiO_2$/$MoS_2$-※ mC represents the charge density of CoP photodeposition (※ mC/$cm^2$). In this paper, if not otherwise specified, Si/Co-NCNHP-$TiO_2$/$MoS_2$ is denoted as Si/Co-NCNHP-$TiO_2$/$MoS_2$-200 mC.

**Table S1** R, $R_s$, $R_{ct1}$ and $R_{ct2}$ of Si/Co-NCNHP-$TiO_2$/CoP, Si/Co-NCNHP-$TiO_2$, Si/$TiO_2$/CoP, Si/$TiO_2$ and Si/CoP.

| | $R_s$ (Ω) | $R_{ct1}$ (Ω) | $R_{ct2}$ (Ω) | $R_{ct2}/R_{ct1}$ | R (Ω) |
|---|---|---|---|---|---|
| $Si_p$/CoP | 6.23 | 8753 | 4512 | 0.52 | 13271.23 |
| $Si_p$/$TiO_2$ | 19.29 | 2254 | $3.287\times10^{19}$ | $1.46\times10^{16}$ | $3.29\times10^{19}$ |
| $Si_p$/$TiO_2$/CoP | 26.16 | 869.6 | 333.3 | 0.38 | 1229.06 |
| $Si_p$/Co-NCNHP-$TiO_2$ | 15.1 | 62.05 | 1177 | 18.97 | 1254.15 |
| $Si_p$/Co-NCNHP-$TiO_2$/CoP | 5.634 | 11.01 | 6.685 | 0.61 | 23.329 |

$R=R_s+ R_{ct1}+ R_{ct2}$, $R_s$ represents the series resistance, $R_{ct1}$ represents the charge transfer resistance between the heterogeneous interfaces inside the electrode, and $R_{ct2}$ represents the charge transfer resistance between the electrode and the electrolyte.

**Table S2** Summary of PEC performance of Si photocathodes coated with earth-abundant catalysts.

| Photocathode | Onset potential (V vs RHE) | Photocurrent density at 0 V vs RHE ($mA \cdot cm^{-2}$) | Stability | Electrolyte | Ref. |
|---|---|---|---|---|---|
| **Si/Co-NCNHP-$TiO_2$/CoP** | **0.409** | **-23.04** | **144 h** | **0.5 M $H_2SO_4$** | **This work** |
| **Si/Co-NCNHP-$TiO_2$/$WS_2$** | **0.297** | **-11.7** | **120 h** | **0.5 M $H_2SO_4$** | |
| **Si/Co-NCNHP-$TiO_2$/$MoS_2$** | **0.395** | **-19.72** | **88 h** | **0.5 M $H_2SO_4$** | |
| Si/$TiO_2$/$NiO_x$ | 0.42 | - 1.48 | >5 h | Phosphate buffer (pH=7.00) | [1] |
| Si/$NiCoSe_x$ | 0.25 | -37.5 | 2 h | 0.5 M $H_2SO_4$ | [2] |
| Si/$TiO_2$/$MoS_2$ | 0.18 | -10 | >15 h | 1 M KOH | [3] |
| $n^+$p-Si/$Al_2O_3$/$MoS_2$ | 0.4 | 35.6 | 120 h | 1 M $HClO_4$ | [4] |
| Si/C/$TiO_2$/Ni–Mo | 0.35 | -17.87 | 2 h | 1 M KOH | [5] |
| Si/$TiO_2$/$MoS_2$ | 0.46 | -33.7 | 150 h | 0.5 M $H_2SO_4$ | [6] |
| Si/Ti/NiFe(1:4) LDH | 0.3 | -7 | 24 h | 1 M KOH | [7] |
| Si/$TiO_2$/WP | 0.27 | −15 | 110 h | 1 M KOH | [8] |
| $n^+$p-Si/Ti/Co-W-S | 0.36 | 30.4 | 144 h | 1 M $HClO_4$ | [9] |
| Si-$TiO_2$–$MoS_2$/Rh–P | 0.43 | -24.1 | >1 h | 0.5 M $H_2SO_4$ | [10] |
| Si/CN/$TiO_2$/NiCoP | 0.42 | -19.87 | 3 h | 1 M KOH | [11] |
| Si/$MoS_{1.75}P_{0.25}$ | 0.29 | -23.8 | 2 h | 0.5 M $H_2SO_4$ | [12] |
| Si/CuCl–Tu | 0.15 | -2.7 | 16 h | 0.2 M phosphate buffer (pH∼7) | [13] |
| $n^+$p-Si/Ti/$NiP_2$ | 0.41 | 12 | 6 | 0.5 M $H_2SO_4$ | [14] |
| Si/$SnS_2$/$MoS_2$ | 0.23 | -23.8 | 2.2 | 0.5 M $H_2SO_4$ | [15] |

**Not:** The explanation of the relationship between reducing the light reflection and increasing the photocurrent density.

Generally, the PEC water splitting process is made up of the following three steps: 1) photoexcitation of electron–hole pairs in the semiconductor, 2) separation and migration of photoinduced electron–hole pairs, and 3) oxidation and reduction of surface water by photogenerated holes and electrons to produce $O_2$ and $H_2$, respectively. Meanwhile, a photon absorbed by semiconductor, which energy is greater than the band gap, can generate an electron-hole pair. Therefore, increasing the light absorption of semiconductor can generate more electron-hole pairs in the semiconductor. Equations for evaluating photocurrent density ($J_{ph}$) are as follows.

$$J_{ph} = J_{abs} \times \eta_{seperation} \times \eta_{injection} \quad \text{(S1)}$$

$$J_{abs} = \frac{q}{hc}\int_{\lambda_1}^{\lambda_2} \lambda \varphi_\lambda \eta_{abs} d_\lambda \quad \text{(S2)}$$

Where $J_{abs}$ is the photon adsorption rate expressed as the photocurrent density, $q$ is the charge of an electron, $h$ is the Plank constant, $c$ is the light speed, $\varphi_\lambda$ is the photon flux of the AM 1.5 G solar spectrum, $\eta_{abs}$ is the light absorption efficiency, $\eta_{seperation}$ is the separation efficiency of photogenerated carriers, and $\eta_{injection}$ is the injection efficiency of photogenerated carriers into electrolyte. It can be seen from equations (S1) and (S2) that the photocurrent density is directly proportional to the light absorption. Therefore, the antireflective structure can increase the light absorption, and then enhance the photocurrent density.

## References


1 A. Kawde, A. Annamalai, L. Amidani, M. Boniolo, W.L. Kwong, A. Sellstedt, P. Glatzel, T. Wågberg, J. Messinger, *Sustain. Energy Fuels*, 2018, **2**, 2215–2223.

2 H. Zhang, Q. Ding, D. He, H. Liu, W. Liu, Z. Li, B. Yang, X. Zhang, L. Lei, S. Jin, *Energy Environ. Sci.*, 2016, **9**, 3113–3119.

3 S.E. Jun, S. Hong, S. Choi, C. Kim, S.G. Ji, I.J. Park, S.A. Lee, J.W. Yang, T.H. Lee, W. Sohn, J.Y. Kim, H.W. Jang, *Small*, 2021, **17**, 2103457.

4 R. Fan, J. Mao, Z. Yin, J. Jie, W. Dong, L. Fang, F. Zheng, M. Shen, *ACS Appl. Mater. Interfaces*, 2017, **9**, 6123–6129.

5 X. Sun, J. Jiang, Y. Yang, Y. Shan, L. Gong, M. Wang, *ACS Appl. Mater. Interfaces*, 2019, **11**, 19132–19140.

6 W. Xun, Y. Wang, R. Fan, Q. Mu, S. Ju, Y. Peng, M. Shen, *ACS Energy Lett.*, 2020, **6**, 267–276.

7 J. Zhao, L. Cai, H. Li, X. Shi, X. Zheng, *ACS Energy Lett.*, 2017, **2**, 1939–1946.

8 F. Li, Y. Yuan, X. Feng, J. Liu, S. Chen, Y. Lin, Y. Sun, H. Chen, L. Zhao, X. Song, P. Zhang, L. Gao, *ACS Appl. Mater. Interfaces*, 2021, **13**, 20185–20193.

9 R. Fan, G. Huang, Y. Wang, Z. Mi, M. Shen, *Appl. Catal. B Environ.*, 2018, **237**, 158–165.

10 Z. Chen, Y. Li, L. Wang, Y. Bu, J.-P.P. Ao, *J. Mater. Chem. A.*, 2021, **9**, 9157–9164.

11 X. Sun, C. Liu, P. Zhang, L. Gong, M. Wang, *J. Power Sources*, 2020, **484**, 229272.

12 C.J. Chen, V. Veeramani, Y.H. Wu, A. Jena, L.C. Yin, H. Chang, S.F. Hu, R.S. Liu, *Appl. Catal. B Environ.*, 2020, **263**, 118259.

13 P. Wang, Z. Yin, L. Gao, H. Li, T. Zhang, Q. Shen, J. Lv, Y. Yao, W. Luo, Z. Zou, *J. Energy Chem.*, 2020, **40**, 75–80.

14 F. Chen, Q. Zhu, Y. Wang, W. Cui, X. Su, Y. Li, *ACS Appl Mater. Interfaces*, 2016, **8**, 31025–31031.

15 A. Jena, K. Pichaimuthu, G. Leniec, S.M. Kaczmarek, H. Chang, C. Su, S.-F. Hu, R.-S. Liu, *ACS Appl. Mater. Interfaces*, 2022, **14**, 39896–39906.